The Retinoblastoma family member p107 regulates the rate of progenitor commitment to a neuronal fate

Jacqueline L. Vanderluit, Crystal A. Wylie, Kelly A. McClellan, Noel Ghanem, Andre Fortin, Steve Callaghan, Jason G. MacLaurin, David S. Park, and Ruth S. Slack

Department of Cellular and Molecular Medicine, Ottawa Health Research Institute, Neuroscience Program, University of Ottawa, Ottawa, Ontario K1H 8M5, Canada

The Retinoblastoma protein p107 regulates the neural precursor pool in both the developing and adult brain. As p107-deficient mice exhibit enhanced levels of Hes1, we questioned whether p107 regulates neural precursor self-renewal through the repression of Hes1. p107 represses transcription at the Hes1 promoter. Despite an expanded neural precursor population, p107-null mice exhibit a striking reduction in the number of cortical neurons. Hes1 deficiency rescues neurosphere numbers in p107-null embryos. We find that the loss of a single Hes1 allele in vivo restores the number of neural precursor cells at the ventricular zone. Neuronal birthdating analysis reveals a dramatic reduction in the rate of neurogenesis, demonstrating impairment in $p107^{-/-}$ progenitors to commit to a neuronal fate. The loss of a single Hes1 allele restores the number of newly generated neurons in p107-deficient brains. Together, we identify a novel function for p107 in promoting neural progenitor commitment to a neuronal fate.

Introduction

Cell cycle genes and specifically those genes that regulate the G1/S transition have been shown to play an important role in regulating the neural precursor population. Members of the cyclin-dependent kinase inhibitor (CDKI) family have received much of the attention. CDKIs, $p21^{Cip1}$, and $p27^{Kip1}$ negatively regulate embryonic and adult neural precursor proliferation (Doetsch et al., 2002; Kippin et al., 2005). Bmi-1 promotes self-renewing cell division in both hematopoeitic and neural precursors through the transcriptional repression of CDKIs, $p16^{Ink4a}$, and $p19^{Arf}$ (Molofsky et al., 2003, 2005). However, cell cycle regulators impacting the neural precursor population are not only restricted to CDKIs (McClellan and Slack, 2006). We have recently shown that the Retinoblastoma (Rb) family member p107, an inhibitor of the cell cycle G1/S transition, negatively regulates the neural precursor pool in the developing and adult brain by regulating self-renewal (Vanderluit et al., 2004).

Correspondence to Ruth S. Slack: rslack@uottawa.ca

J.L. Vanderluit's present address is Division of BioMedical Sciences, Faculty of Medicine, Memorial University of Newfoundland, St. John's, Newfoundland A1B 3V6, Canada.

Abbreviations used in this paper: BS, binding site; CDKI, cyclin-dependent kinase inhibitor; IZ, intermediate zone; PCNA, proliferating cell nuclear antigen; PH3, phosphohistone H3; pRb, Rb protein; Rb, Retinoblastoma; SVZ, sub-VZ; VZ, ventricular zone.

p107 has been shown to function by interacting with E2F transcription factors (preferentially E2F4) to repress the transcription of genes required for cell cycle progression (Stevaux and Dyson, 2002). Distinct from other Rb family members, p107 is only expressed in cycling neural precursor cells in the ventricular zone (VZ; Jiang et al., 1997).

The Notch–Hes pathway is necessary for self-renewing cell division and, thus, maintenance of the neural precursor population (Ishibashi et al., 1995; Ohtsuka et al., 2001; Hitoshi et al., 2002; Hatakeyama et al., 2004). Whereas the deletion of either Notch1, Hes1, or Hes1 and Hes5 causes premature differentiation of embryonic neural precursors, resulting in their depletion (Ishibashi et al., 1995; Ohtsuka et al., 2001; Hitoshi et al., 2002), the overexpression of activated Notch1 or Hes1 results in an expansion of neural precursor numbers (Ishibashi et al., 1994). Hes1 and Hes5 inhibit differentiation by repressing the expression of the proneural genes *Mash1*, *NeuroD*, and *Math1* (Sasai et al., 1992; Ishibashi et al., 1995). Because the Notch–Hes signaling pathway is crucial for neural precursor self-renewal and inhibition of premature differentiation, we asked whether the cell cycle protein p107 may be regulating the neural precursor population and progenitor differentiation by the repression of Hes1.

In this study, we demonstrate that the p107-mediated regulation of neural precursor number occurs through the repression

The Journal of Cell Biology, Vol. 178, No. 1, July 2, 2007 129–139
http://www.jcb.org/cgi/doi/10.1083/jcb.200703176

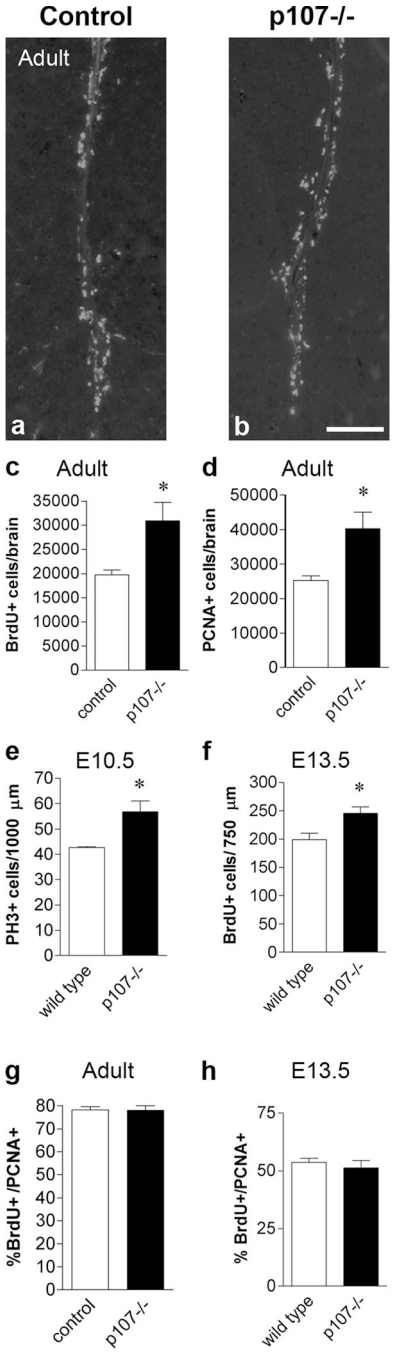

Figure 1. **Increased numbers of progenitor cells in the embryonic and adult p107$^{-/-}$ brains in vivo.** (a–c) To assess the size of the neural progenitor population in the adult brain, mice received intraperitoneal injections of BrdU to label proliferating cells over a 10-h period. BrdU-positive cell counts through the lateral ventricles showed a 50% increase in the number of progenitors in p107$^{-/-}$ brains ($n = 4$) in comparison with wild type ($n = 3$). (d) The adult progenitor population was also assessed by immunohistochemistry for PCNA. Similar to our BrdU incorporation study, p107-deficient brains had a comparable increase in PCNA^{+} cells along the ventricles. (e) To quantify the number of proliferating progenitors in E10.5 brains, we used an antibody to phosphohistone H3 (PH3), a marker of cells in M phase of the cell cycle. PH3-positive cells were counted along the lateral ventricles in three representative sections of wild-type ($n = 3$) and p107$^{-/-}$ ($n = 3$) brains. (f) A 2-h BrdU pulse was used to label progenitors in S phase in E13.5 brains. BrdU-positive cells were counted in four representative regions of the forebrain in wild-type ($n = 4$) and p107$^{-/-}$ ($n = 3$) embryos. Note that at adult and embryonic ages, p107$^{-/-}$ mice had significantly more proliferating cells along the lateral ventricle than wild-type mice. (g and h) To assess whether in vivo cell cycle kinetics were different in p107$^{-/-}$ neural progenitors, we compared the size of the S-phase fraction by immunolabeling for BrdU and PCNA in adult (g) and E13.5 wild-type and p107$^{-/-}$ cortices (h). Quantification of BrdU+ cells (S-phase fraction) was compared with the total proliferating population (PCNA^{+}). After 10.5 h of cumulative BrdU labeling, 78.2% and 78% of the total proliferating populations in wild-type and p107$^{-/-}$ cortices were BrdU^{+}, respectively, indicating similar cell cycle kinetics. At E13.5 after a 2-h BrdU pulse, 53.6% and 51.2% of the total proliferating populations in wild-type and p107$^{-/-}$ were BrdU^{+}, respectively. Means were statistically analyzed using a t test, and differences were assessed at *, $P < 0.05$. Error bars represent SEM. Bar, 100 µm.

of *Hes1* transcription. Hes1 is elevated in p107-deficient brains. Loss of a single *Hes1* allele restores the neural precursor population to wild-type levels both in vitro and in vivo. Despite the expanded progenitor population, p107- deficient brains exhibit a reduction in the number of cortical neurons that cannot be accounted for by apoptosis. Short- and long-term BrdU labeling studies revealed a striking defect in the rate at which p107-null progenitors commit to a neuronal fate. Loss of a single Hes1 allele on a p107-null background rescues the number of neurons born during cortical development. Together, these results identify that the mechanism by which p107 regulates both neural precursor self-renewal and differentiation is through regulation of the Notch–Hes1 signaling pathway. In summary, we identify a novel function for p107, a cell cycle regulatory protein, in controlling the onset of differentiation.

Results

p107 regulates the size of the neural precursor population

To determine the temporal requirement for p107 in regulating the neural precursor population, we counted the number of proliferating precursors in the brains of mice at three different ages: in adults and in embryos at embryonic days (E) 10.5 and 13.5. Using antibodies to label cells in the cell cycle (proliferating cell nuclear antigen [PCNA], which labels cells in all phases of the cell cycle; phosphohistone H3 [PH3], which labels cells in M phase; and BrdU, which gets incorporated during S phase), we demonstrate an increase in the proliferating precursor population in p107-null mice. Adult p107-null mice have a 50% increase in the number of precursors, as demonstrated by both cumulative BrdU labeling of proliferating progenitor cells and PCNA immunostaining (Fig. 1, a–d). Similarly, at both embryonic time points E10.5 and 13.5, p107-null embryos had more precursor cells (Fig. 1, e and f). The difference is most pronounced in adult mice when proliferation rates are slower, with a cell cycle time of ~12.7 h (Morshead and van der Kooy, 1992). These studies demonstrate that p107 mutants have an expanded precursor population.

As the increased number of neural precursor cells in p107-deficient mice could be the result of an increased total population or an enhanced rate of cell division, we assessed the proliferative index in embryonic and adult wild-type and p107$^{-/-}$ mice. Double immunohistochemistry for BrdU and PCNA was performed on adult brains after 10.5 h of cumulative BrdU labeling and on embryonic brains after a 2-h pulse of BrdU. The number of cells that entered S phase (BrdU^{+} cells)

was compared with the total proliferating population (PCNA-expressing cells) in wild-type and p107$^{-/-}$ mice. A more rapid cell cycle time in p107 knockouts would result in a greater percentage of cells in S phase (Cayre et al., 2005). In adult wild-type mice, 78.2 ± 1.4% of the proliferating population incorporated BrdU, whereas in p107$^{-/-}$ mice, 78.0 ± 1.9% were BrdU positive (Fig. 1 g). After a 2-h BrdU pulse at E13.5, 53.6 ± 1.8% of wild-type and 51.3 ± 3.2% of p107$^{-/-}$ cells incorporated BrdU (Fig. 1 h). Thus, comparable proliferative indices in adult and embryonic ages indicate similar cell cycle times. Therefore, the increased number of total progenitor cells at each stage of development represents an overall expansion of the precursor population in p107$^{-/-}$ mice. This increase in total precursor number is consistent with our previous studies revealing that p107-deficient animals exhibit elevated levels of the Notch1–Hes1 pathway and increased stem cell self-renewal (Vanderluit et al., 2004). As the Notch1 pathway has been shown to play an essential role in stem cell self-renewal (Hitoshi et al., 2002), our expanded precursor population in p107 deficiency is consistent with an increase in the Notch–Hes1 pathway. Therefore, we asked whether the expanded precursor population in p107-deficient mice is the result of the deregulation of Hes1.

Deregulated Hes1 expression in p107$^{-/-}$ neural precursors

Because we have previously demonstrated the deregulation of Notch signaling in p107-deficient neural precursors (Vanderluit et al., 2004), we examined the expression of Notch targets Hes1 and Hes5 in p107 deficiency. Hes1 and Hes5 are basic helix-loop-helix transcription factors that act downstream of Notch to regulate neural precursor self-renewal (Kageyama et al., 2005). In situ hybridization revealed elevated levels of *Hes1* transcript in cells of the VZ in p107$^{-/-}$ mice at E14.5 (Fig. 2, a and b). Quantitative real-time RT-PCR further demonstrated increased *Hes1* mRNA in embryonic p107-deficient cortices (Fig. 2 c). In contrast to *Hes1* expression, no difference in *Hes5* mRNA was detected by in situ hybridization or real-time RT-PCR (Fig. 2, d–f). An examination of Hes1 protein by Western blotting also revealed enhanced expression in neurospheres derived from p107$^{-/-}$ embryos (Fig. 2 g). Although both Hes1 and Hes5 are Notch1 targets, only *Hes1* is deregulated in p107$^{-/-}$ mice. The selective deregulation of *Hes1* expression leads us to question whether p107 could regulate *Hes1* transcription.

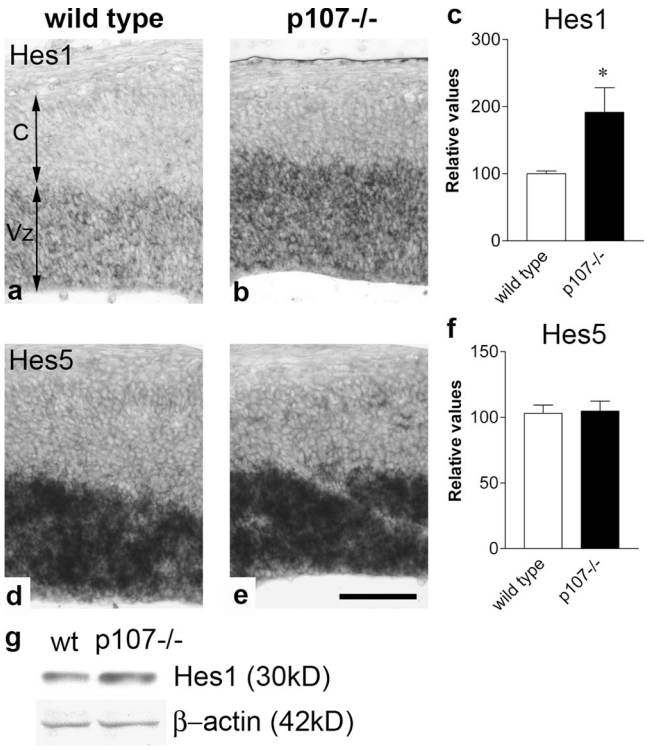

Figure 2. **Hes1 expression is deregulated in p107$^{-/-}$ precursor cells.** (a and b) In situ hybridization revealed higher levels of Hes1 mRNA in the VZ of E14.5 p107$^{-/-}$ mice versus wild-type littermates. (c) Elevated levels of Hes1 mRNA were also demonstrated by real-time RT-PCR on whole cortices from E12.5 wild-type ($n = 4$) and p107$^{-/-}$ ($n = 4$) embryos. (d–f) In contrast, no difference was observed in the levels of Hes5 mRNA between wild type and p107$^{-/-}$ by in situ hybridization (d and e) or real-time RT-PCR (f). (g) Neuroepithelia from E10.5 wild-type (wt) and p107$^{-/-}$ mice were cultured as neurospheres. Protein was isolated from the neurospheres for Western blot analysis. A representative Western blot initially probed with an antibody to Hes1 and then reprobed with an antibody to actin to verify equal quantities of protein was loaded per lane. The experiment was performed in triplicate. Vz, ventricular zone; C, cortical plate and IZ. Means were analyzed by a *t* test with *, $P < 0.05$. Error bars represent SEM. Bar, 50 μm.

p107 represses Hes1 promoter activity

Because in situ hybridization and real-time RT-PCR reveal that *Hes1* is deregulated in p107$^{-/-}$ neural precursors, we questioned whether p107 could regulate *Hes1* transcription. To determine whether the *Hes1* promoter is responsive to p107, we used a luciferase promotor assay. The *Hes1* promoter (~1,500 bp) was inserted into a pGL3-Basic reporter vector containing the luciferase gene (B-Hes1; Fig. 3 a). This construct was transfected into HEK 293A cells along with 3 μg of a p107 expression vector or Rb expression vector as a control. Cotransfection of 3 μg p107 resulted in a 2.5-fold reduction in *Hes1* promoter activity (Fig. 3 b). This repression was dose dependent because a further increase in p107 (10 μg) resulted in a >10-fold repression. In contrast, protein Rb (pRb) did not repress *Hes1* promoter activity. These results demonstrate that p107 represses *Hes1* promotor activity.

Because p107 regulates transcription by interacting with E2F transcription factors, we asked whether E2Fs were required for p107-mediated repression. The *Hes1* promotor was analyzed, and three putative E2F-binding sites (BSs [E2F-BS]) were found at positions −560, 161, and 398 bp relative to the transcription start site (Fig. 3 a). To test whether E2Fs were required for p107-mediated repression, we deleted all three BSs from the *Hes1* promotor (Hes1-3xBS). Cotransfection of the Hes1-3xBS construct with the p107 expression vector resulted in pronounced repression of luciferase activity (Fig. 3 c). These results demonstrate that p107-mediated repression of the *Hes1* promotor occurs indirectly, independent of these E2F sites. Nevertheless, our results showing decreased levels of *Hes1* transcript and protein combined with p107-mediated repression of the *Hes1* promoter demonstrate that p107 is required in the neural precursor population for the repression of *Hes1*.

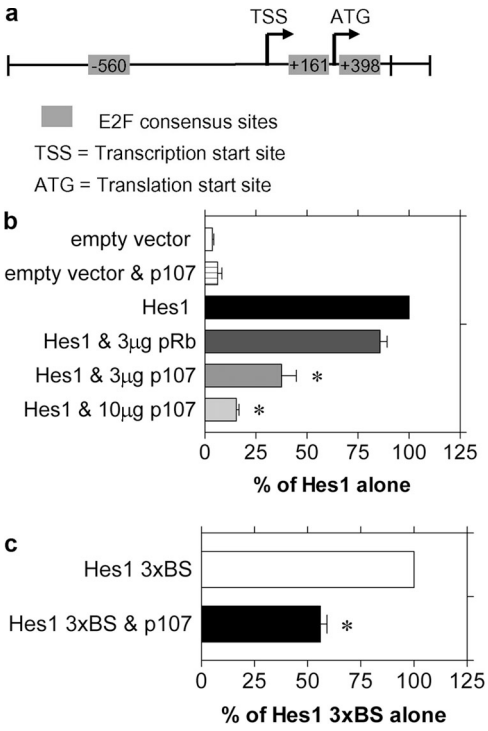

Figure 3. **p107 represses Hes1 promoter activity.** (a) Diagram of the Hes1 promotor (~1,500 bp) containing three putative E2F-BSs at positions −560, 161, and 398 bp relative to the transcriptional start site. (b) Luciferase assay of HEK 293A cells transfected with the pGL3B-Luc Hes1 promoter constructs and 3 μg of expression vectors containing either Rb or p107. Rb has no effect on Hes1 promoter activity, whereas 3 μg p107 represses Hes1 promoter activity by a factor of 2.5, and 10 μg p107 represses 10-fold. (c) Transfection of the pGL3B-Luc Hes1-3xBS promoter (E2F-binding mutant) with p107 still resulted in the repression of promoter activity, suggesting that p107 represses Hes1 transcription through an E2F-independent mechanism. Experiments were performed in triplicate. Means were statistically analyzed by one-way analysis of variance followed by Tukey's individual comparison of the means. Error bars represent SEM. *, $P < 0.05$.

p107 regulates neural precursor numbers by the repression of Hes1

To ask whether p107 regulates the neural precursor population by the repression of *Hes1*, we interbred p107-deficient mice with animals carrying a null mutation for *Hes1*. We hypothesized that if p107 regulated neural precursor cells by controlling the levels of Hes1, the loss of one or more alleles of *Hes1* in p107-null mice should partially or completely restore the expanded precursor population to wild-type levels. Conversely, if p107 acted through an independent pathway, the number of neural precursors would not be affected by the loss of Hes1, as seen in wild-type cells. Because $Hes1^{-/-}$ mice are embryonic lethal after E12.5, embryos were taken at E10.5 (Ishibashi et al., 1995). The neuroepithelia from each embryo was dissociated into a single-cell suspension, cells were plated at clonal density, and, after 7 d, neurospheres were counted. Cultures from p107-null mice produced substantially more neurospheres than cultures from all other genotypes (Fig. 4). Consistent with previous findings (Ohtsuka et al., 2001), the loss of Hes1 alone had no effect on neural precursor numbers from wild-type animals, whereas the absence

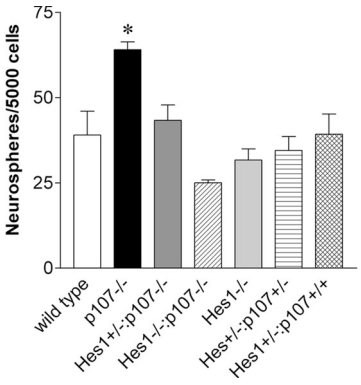

Figure 4. **Loss of Hes1 restores the number of neural precursors to wild-type levels in $p107^{-/-}$ embryos.** Quantification of neurospheres revealed that $p107^{-/-}$ cultures produced significantly more neurospheres than all of the other genotypes, including $Hes1^{-/-}$:$p107^{-/-}$ and $Hes1^{+/-}$:$p107^{-/-}$. Therefore, a reduction in Hes1 expression in $p107^{-/-}$ mice restores the number of neural precursors back to wild-type levels (wild type, $n = 3$; $p107^{-/-}$, $n = 3$; $Hes1^{+/-}$:$p107^{-/-}$, $n = 6$; $Hes1^{-/-}$:$p107^{-/-}$, $n = 5$; $Hes1^{-/-}$, $n = 3$; $Hes1^{+/-}$:$p107^{+/-}$, $n = 4$; $Hes1^{+/-}$:$p107^{+/+}$, $n = 4$). Means were statistically analyzed by one-way analysis of variance followed by Tukey's individual comparison of the means. Error bars represent SEM. *, $P < 0.05$.

of one or both alleles of *Hes1* in p107-deficient precursor cells restored neurosphere numbers to wild-type levels. Together with the demonstration that p107 represses *Hes1* gene expression, these results demonstrate that the expanded neural precursor population in $p107^{-/-}$ embryos results from the deregulation of *Hes1*.

p107 regulates the neural precursor population in vivo through the repression of Hes1

We next questioned whether p107 controlled the size of the neural precursor population in vivo through the repression of *Hes1*. As a result of the embryonic lethality of double mutant mice, we asked whether the loss of a single *Hes1* allele could restore the number of neural precursor cells in p107-null mice to wild-type levels. In adult mice, the precursor population was labeled with BrdU. Counts of BrdU-positive cells in adult brains showed that a reduction in Hes1 could restore the number of proliferating precursors in p107-null mice (Fig. 5 a). PH3 immunohistochemistry of the rapidly dividing E10.5 neural precursors demonstrated that loss of a single *Hes1* allele in p107-null embryos ($Hes1^{+/-}$:$p107^{-/-}$) reduced the number of cells in M phase to levels comparable with the wild type (Fig. 5 b). Similarly, a 2-h BrdU pulse in E13.5 embryos also revealed a reduction in the number of cells in S phase in $p107^{-/-}$ embryos lacking a single *Hes1* allele (Fig. 5 c). Loss of a single *Hes1* allele in $p107^{-/-}$ mice restored the number of proliferating cells to wild-type levels at all three developmental time points. In contrast, loss of a single *Hes1* allele on a wild-type background ($Hes1^{+/-}$) did not result in a reduction in the number of proliferating cells (Fig. 5 c). These results demonstrate that p107 regulates the neural precursor population by controlling the levels of Hes1 in progenitor cells.

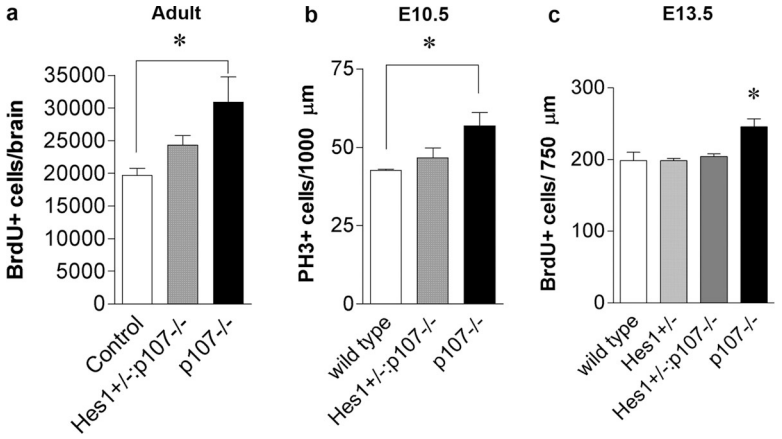

Figure 5. **p107 regulates the neural precursor population through the repression of Hes1.** (a) Adult mice received intraperitoneal injections of BrdU to label proliferating cells over a 10-h period. BrdU-positive cells were counted in every 10th section through the forebrains of wild-type ($n = 3$), Hes1$^{+/-}$:p107$^{-/-}$ ($n = 4$), and p107$^{-/-}$ ($n = 5$) mice. (b) Proliferating progenitors in E10.5 brains were identified by PH3 immunohistochemistry. PH3-positive cells were counted in three representative sections of wild-type ($n = 3$), Hes1$^{+/-}$:p107$^{-/-}$ ($n = 3$), and p107$^{-/-}$ ($n = 3$) brains. (c) A 2-h BrdU pulse labeled proliferating progenitors in E13.5 brains. BrdU-positive cells were counted in four representative regions of the brain in wild-type ($n = 4$), Hes1$^{+/-}$:p107$^{-/-}$ ($n = 4$), Hes1$^{+/-}$ ($n = 4$), and p107$^{-/-}$ ($n = 3$) embryos. Note that loss of a single Hes1 allele restored the numbers of progenitor cells to wild-type levels in p107$^{-/-}$ mice at embryonic and adult ages. Means were statistically analyzed by one-way analysis of variance followed by Tukey's individual comparison of the means. Error bars represent SEM. *, $P < 0.05$.

p107 deficiency leads to a decreased number of mature neurons

The expanded neural precursor numbers in p107$^{-/-}$ mice lead us to question whether the number of cortical neurons was also affected. Specifically, we asked whether the expanded precursor population leads to increased neurogenesis. Immunohistochemistry with NeuN, a marker for mature central nervous system neurons, revealed a significant reduction ($P < 0.05$) in the number of NeuN-expressing cells in p107$^{-/-}$ cortices (Fig. 6, a–c). The decreased number of cortical neurons is further demonstrated by a reduction in the overall size/thickness of the cortex (Fig. 6, d and f), whereas measurements of the VZ did not reveal any differences between p107$^{-/-}$ mice and wild type at E18.5 (Fig. 6 e). Because p107-deficient mice exhibit a reduction in the total number of cortical neurons despite an expanded progenitor pool, we questioned whether p107 was required for the survival of cortical neurons.

To determine whether an increase in cell death was responsible for the reduction in cortical neuron numbers in p107-deficient brains and at what stage in development cells were dying, we counted the number of apoptotic cells in the VZ/sub-VZ (SVZ), the intermediate zone (IZ), and in the cortical plate and marginal zone. Apoptotic cells were identified by immunohistochemistry for active caspase-3 and Hoechst nuclear staining in E13.5 embryonic brains (Fig. 7, a–f). The number of apoptotic cells in the brains of wild-type and p107$^{-/-}$ mice was low, with less than one cell per 1,000-μm^2 area (Fig. 7 h). As a result of the low frequency of apoptotic cells, counts were performed in 12 sections throughout the telencephalon in both left and right hemispheres, and the total number of apoptotic cells was compared between genotypes (Fig. 7 g). A twofold increase in the number of apoptotic cells was observed only in the VZ/SVZ of p107-null brains, whereas no differences were observed in the IZ or cortical plate/marginal zone. An increase in cell death in the p107 mutant VZ/SVZ suggests that newly committed neurons may be dying in the VZ before they initiate migration.

To identify at which stage in progenitor cell development cells were dying, double immunolabeling was performed with antibodies to active caspase-3 and Nestin (progenitor cell marker), doublecortin (migratory neuroblast), and βIII-tubulin (Tuj1, an early neuronal marker). Because the increase in apoptotic cells is only in the VZ/SVZ, we counted the double-labeled cells in this region. At E13.5, most cells were double labeled with active caspase-3/Nestin (Fig. 7, a–f), suggesting that p107 affects the survival of uncommitted progenitor cells. No double labeling was detected with doublecortin or Tuj1 in any of our samples, ruling out the possibility that p107 deficiency results in enhanced cell death in newly committed neuroblasts. As apoptosis progresses, dying cells will lose their cell type–specific markers; thus, some pyknotic cells did not colabel with Nestin or any other marker examined. The colabeling of apoptotic cells with caspase-3 and Nestin is consistent with the interpretation that cell death is occurring in uncommitted progenitor cells in the

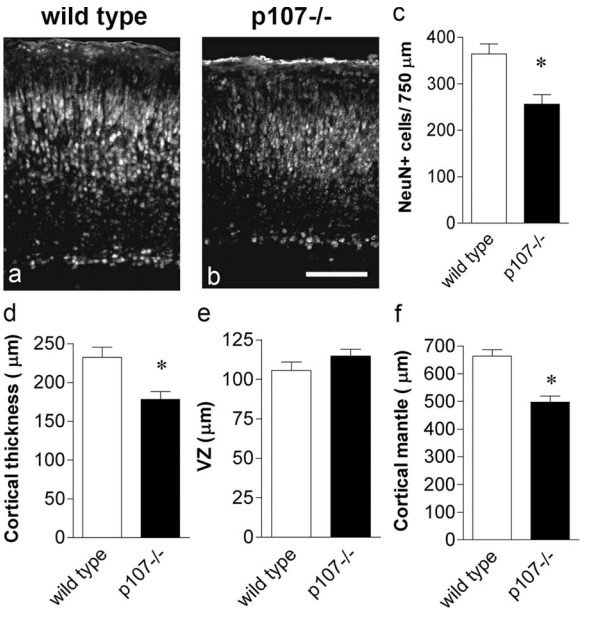

Figure 6. **Reduced neuronal numbers in the developing cortex of p107$^{-/-}$ embryos.** (a–c) To assess neuronal differentiation, coronal brain sections were stained for the neuronal marker NeuN. Immunohistochemistry on E18.5 brains revealed a reduction in the number of NeuN-positive cells in p107$^{-/-}$ cortices. (d–f) Brain measurements at E18.5 revealed significantly thinner cortices and cortical mantle but no change in the size of the VZs in p107$^{-/-}$ embryos (wild type, $n = 4$; p107$^{-/-}$, $n = 4$). Means for each measurement was assessed with a *t* test. Error bars represent SEM. *, $P < 0.05$. Bar, 100 μm.

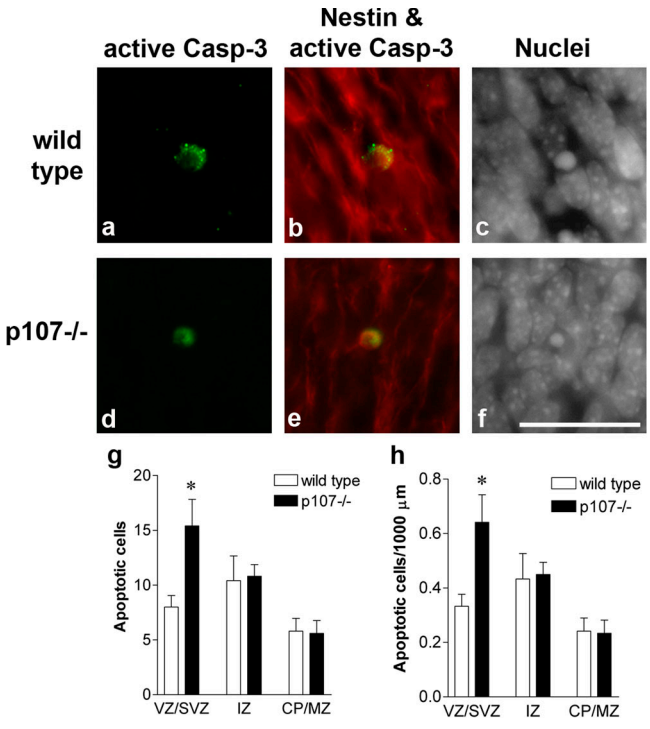

Figure 7. **Reduced neuronal numbers is not the result of enhanced apoptosis in the cortical plate.** (a–f) To determine whether p107 was required for the survival of postmitotic neurons in the cortical plate, we counted the number of apoptotic cells in the developing cortex of E13.5 embryos. Apoptotic cells were identified by active caspase-3 immunohistochemistry and Hoechst nuclear staining. (b and e) Within the SVZ/VZ, colabeling of active caspase-3 and Nestin identified the majority of dying cells as uncommitted progenitors. (g) Total apoptotic cells were counted across 12 representative sections in both left and right hemispheres through the telencephalon. Cell counts revealed an increase in apoptosis in the VZ/SVZ of $p107^{-/-}$ embryos but not in the developing cortex (wild type, $n = 4$; $p107^{-/-}$, $n = 4$). (h) The number of apoptotic cells per 1,000-µm length along the ventricle and up through to the pial layer showed an extremely low frequency of cell death per counting area. Mean counts were assessed by a two-way analysis of variance followed by Bonferroni's individual comparison of means. CP, cortical plate; MZ, marginal zone. Error bars represent SEM. *, $P < 0.05$. Bar, 25 µm.

VZ/SVZ. The increase in apoptosis in the VZ/SVZ did not reveal any death of newly committed neurons. In conclusion, these studies show that the absence of p107 results in the increased cell death of Nestin- expressing progenitor cells.

p107 controls neural progenitor commitment to a differentiated fate in vivo

As the increased apoptosis in the VZs of p107-null mice is caused by the death of uncommitted Nestin-expressing progenitor cells and the rate of cell death was still very low, we questioned whether the absence of p107 may result in a defect in the rate of neuronal commitment. To address this question, we performed neuronal birthdating assays using a BrdU protocol to label cells undergoing terminal mitosis at the time of BrdU injection. Neuronal birthdating is based on the demonstration that neurogenesis occurs between E12 and 17, during which cohorts of neural precursors are born (neuronal commitment) at distinct time points and migrate out of the VZ to form the layers of the cortex (Caviness, 1982; Caviness et al., 1995; Takahashi et al., 1999). A single BrdU injection labels all cells in S phase, but only neural precursors undergoing terminal mitosis retain the BrdU label. Therefore, BrdU birthdating provides a quantitative analysis of cells that commit to a neuronal fate, undergo terminal mitosis, and migrate to their ultimate destination in the cerebral cortex. Accordingly, pregnant dams were injected with BrdU at E13.5 (Takahashi et al., 1999), the time at which deep layer cortical neurons are generated. Embryos were collected 5 d after injection at E18.5. BrdU cell counts revealed that $p107^{-/-}$ mice (36 ± 5; $n = 5$) had a dramatic twofold reduction in the number of neurons that were born at injection time (E13.5) and reached the cortical plate by E18.5 relative to wild-type littermates (68 ± 9; $n = 4$; Fig. 8, a–c). These results show that there is a decrease in the number of neurons reaching the cortical plate in p107-deficient brains.

Because our examination of cell death did not reveal a loss of newly generated neurons in the cortical plate, we asked whether the reduced neuronal numbers in p107-deficient mice was caused by fewer neurons born at E13.5 (the time of BrdU injection). To address this question, we performed a 24-h BrdU incorporation to measure the rate of neuronal commitment. Pregnant dams were injected at E13.5, embryos were collected 24 h later at E14.5, and the number of strongly labeled BrdU-positive cells were counted (i.e., cells that underwent terminal mitosis at the time of injection). In addition, sections were double stained with PCNA to show that these cells are no longer cycling. Double labeling with BrdU and PCNA revealed that most BrdU-positive cells within the SVZ and IZ were no longer expressing PCNA, indicating that they were newly postmitotic (Fig. 8, d–f). Cell counts of this newly postmitotic population revealed a two-fold reduction in p107-deficient brains compared with wild-type controls (Fig. 8, f and i). These results demonstrate that there is a decrease in the number of newly postmitotic cells leaving the VZ in p107-deficient animals.

We hypothesized that a decrease in the number of newly postmitotic cells migrating out of the VZ/SVZ in p107-deficient mice indicates that p107 may be required for the regulation of neuronal commitment. To test this possibility, we performed the aforementioned 24-h BrdU commitment assay followed by double labeling with BrdU and doublecortin to identify migrating neuroblasts or BrdU and Tuj1, an early panneuronal marker induced just after terminal mitosis. Double labeling revealed that p107-deficient mice exhibited a striking decrease in the number of BrdU-positive cells expressing doublecortin (wild type, 76.7 ± 0.7; and $p107^{-/-}$, 56.1 ± 4.1) and Tuj1 (wild type, 78.3 ± 3.2; and $p107^{-/-}$, 49.5 ± 5.4; Fig. 8, j–o). These findings support a model whereby fewer p107-deficient progenitor cells commit to a neuronal fate, resulting in a twofold reduction in cortical neurons in the brain at E18. In summary, our results reveal that p107 is required for neuronal commitment and promotes the decision to exit the progenitor pool and commit to a neuronal fate.

Because our results show that Hes1 is involved in p107-mediated neural precursor self-renewal and Hes1 functions to maintain the neural precursor population by repressing the expression of proneural genes (Sasai et al., 1992; Ishibashi et al., 1995), we asked whether deregulated Hes1 could account for the defect in neurogenesis in p107-null mice. The loss of a

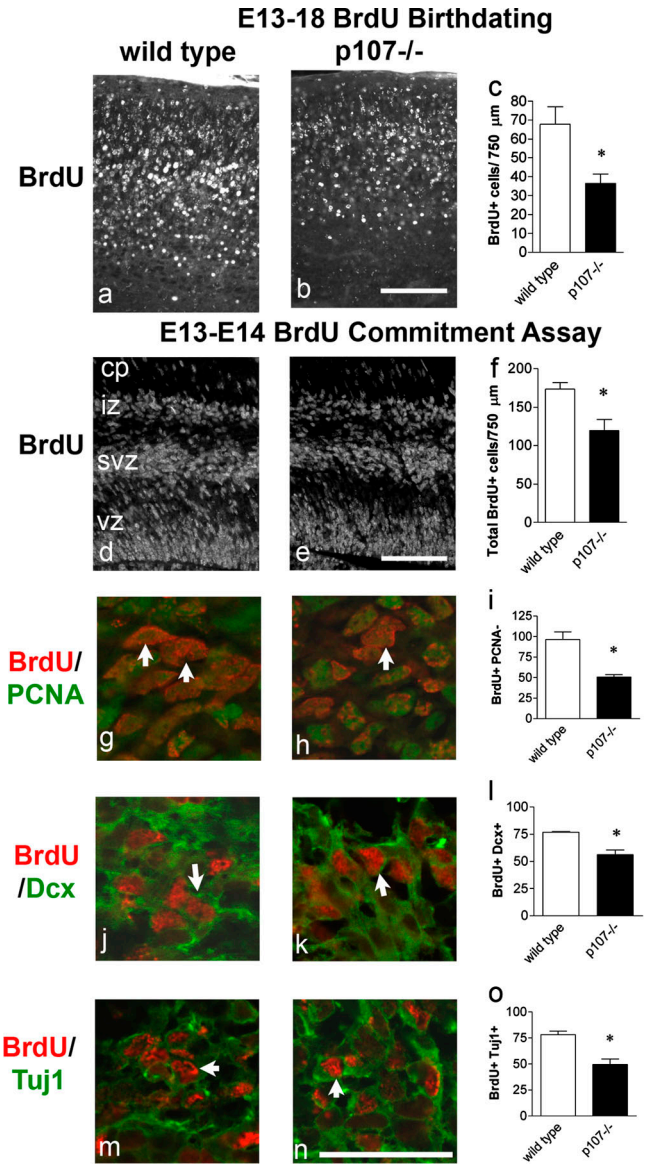

Figure 8. **Defective differentiation in p107$^{-/-}$ neural precursors.** Long-term BrdU birthdating analysis (E13–18) showed a reduction in the number of cells exiting the VZ and arriving in the cortical plate. Pregnant females received an intraperitoneal injection of 20 mg/kg BrdU at gestation day 13.5 (E13.5). Embryos were collected 5 d later at E18.5, and BrdU$^+$ cells were counted in the developing cortices. (a–c) p107$^{-/-}$ embryos had significantly fewer BrdU$^+$ cells in the cortex in contrast to wild-type embryos (wild type, $n = 4$; p107$^{-/-}$, $n = 4$). (d–f) To assess the number of neurons born at E13, short-term BrdU birthdating (E13–14) was performed with pregnant females receiving an intraperitoneal injection of 20 mg/kg BrdU at E13.5, and embryos were collected 24 h later at E14.5. (d and e) Strongly labeled BrdU$^+$ cells were primarily located in the IZ and SVZ. (f) Quantification of the number of strongly labeled BrdU$^+$ cells revealed a significant reduction in p107-deficient brains. (g–i) Double labeling of BrdU and PCNA was performed to assess whether cells had undergone terminal mitosis and exited the cell cycle (i.e., BrdU$^+$ PCNA$^-$ cells; arrows). (j–o) Strongly labeled BrdU$^+$ cells were colabeled with doublecortin (DCX), a marker of migratory cells (j–l), and Tuj1, an early neuronal marker identifying these cells as newly born neurons (m–o). Arrows in j, k, m, and n identify double-labeled cells. The lower number of BrdU-positive cells in the cortex of p107$^{-/-}$ embryos at E18.5 and in the SVZ and IZ at E14.5 despite an expanded precursor population demonstrates a defect in the commitment to a neuronal fate. Means for each measurement was assessed with a *t* test. Error bars represent SEM. cp, cortical plate. *, $P < 0.05$. Bars: (a–e) 100 µm; (g, h, j, k, m, and n) 25 µm.

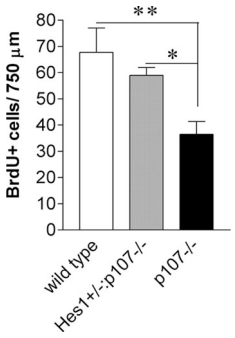

Figure 9. **A reduction in Hes1 restores cortical neurogenesis in p107-deficient brains.** Long-term BrdU birthdating (E13–18) of wild-type ($n = 4$), Hes1$^{+/-}$:p107$^{-/-}$ ($n = 6$), and p107$^{-/-}$ ($n = 4$) embryos revealed that loss of a single Hes1 allele could restore neurogenesis in p107-deficient brains. Means were statistically analyzed by one-way analysis of variance followed by Tukey's individual comparison of the means. Error bars represent SEM. *, $P < 0.05$; **, $P < 0.01$.

single *Hes1* allele could partially restore the rate of neurogenesis by increasing the number of neurons that commit to a neuronal fate at E13.5. Specifically, BrdU birthdating revealed that a reduction in Hes1 could restore the number of neurons born at E13.5 from 37 ± 5 ($n = 4$) in p107$^{-/-}$ to 59 ± 3 ($n = 6$) in Hes1$^{+/-}$:p107$^{-/-}$ comparable with wild-type levels of 68 ± 9 ($n = 4$; Fig. 9). These results highlight that p107 regulates the neural precursor pool by regulating self-renewal and controlling the decision to exit the progenitor pool and commit to a neuronal fate. Furthermore, we show that the mechanisms underlying p107-mediated regulation of the neural precursor population is through repression of the Notch–Hes1 pathway.

Discussion

In this study, we identify a novel role for p107 in regulating the transition from proliferating neural progenitor cell to committed neuroblast. During neural development, p107 regulates the size of the neural precursor pool by limiting self-renewal capacity and promoting the transition from progenitor cell to committed neuroblast. Furthermore, we show that the mechanism by which p107 regulates the neural precursor pool is through repression of Notch–Hes1 signaling.

The cell cycle protein p107 regulates neural precursor self-renewal through the repression of Hes1

In this study, we demonstrate that p107 regulates neural precursor self-renewal through the repression of Hes1. Our previous work has shown that p107-deficient neural precursors have an enhanced self-renewal capacity and that Notch1 and Hes1 are up-regulated (Vanderluit et al., 2004). Because we observed an up-regulation of only Hes1 and not Hes5, we questioned whether p107 might be acting at multiple levels along the Notch–Hes1 pathway. Although promotor analysis reveals that *Hes1* repression is indirect, likely resulting from Notch activation, these experiments set the rationale for using the *Hes1* mutant mice to reduce signaling through the Notch1 pathway. By interbreeding p107 and *Hes1* mutant mice, the defect found in p107 mutant is rescued.

The loss of one or more *Hes1* alleles in p107-deficient mice restores both the size of the neural precursor pool to wild-type levels and the differentiation defect. These results identify a novel mechanism whereby p107, a cell cycle protein, regulates the neural precursor population through the repression of *Hes1*, a gene that inhibits differentiation by repressing proneural gene transcription. Although previous studies have shown that cell cycle inhibitors such as the CDKIs ($p16^{Ink4a}$, $p18^{Ink4c}$, $p19^{Arf}$, $p21^{Cip1}$, and $p27^{Kip1}$) negatively regulate neural precursor proliferation, they function by direct inhibition of the cell cycle machinery (cyclin kinases; Cheng et al., 2000; Doetsch et al., 2002; Molofsky et al., 2003, 2005; Yuan et al., 2004; Kippin et al., 2005). In contrast, p107 regulates the transcription not only of cell cycle genes but also genes that impact the onset of differentiation, such as *Hes1*. Our studies support a novel concept whereby the role of cell cycle genes such as p107 extends beyond regulation of the cell cycle machinery and directly impacts the onset of differentiation in the developing nervous system.

p107 promotes progenitor commitment to a neuronal fate

During cortical development, progenitor cells in the VZ commit to a neuronal fate, undergo terminal mitosis, and commence migration into the cortical plate, where they undergo differentiation. Previously, we demonstrated that p107 regulates neural precursor numbers by limiting self-renewal (Vanderluit et al., 2004). In the present study, we extend these findings to show that p107 has an additional function in controlling this population by regulating commitment to a neuronal fate. p107-deficient mice have an overall reduction in the number of cortical neurons, resulting in considerably smaller brains despite an expansion of the neural precursor population. This was not caused by the increased cell death of committed neurons because no difference in the number of apoptotic cells in the p107-deficient cortical plate was found. Although an increase in apoptosis was observed in the VZ/SVZ of p107-deficient mice, double labeling revealed that these cells coexpressed Nestin, indicating that apoptosis was elevated in uncommitted progenitor cells. Consistent with this, there was no double labeling of VZ/SVZ apoptotic cells with doublecortin or Tuj1, which are markers for newly committed neurons. There is the possibility that newly committed SVZ progenitors may undergo apoptosis before the expression of early commitment markers, but the frequency of apoptotic cells is very low, making this interpretation unlikely.

In further support of a defect in neuronal commitment, we performed a 24-h (E13–14) BrdU labeling analysis, which revealed a substantial reduction in the number of newly committed neurons in p107-deficient brains (Fig. 8). These findings support our long-term birthdating (E13–18) study that demonstrated a twofold decrease in the number of cortical neurons (Fig. 6), further supporting a model whereby fewer neurons are born during the time that neurogenesis takes place in the developing p107-deficient cortex. This demonstrates that p107 promotes progenitor cell commitment to a neuronal fate. Whereas in p107-deficient mice, expanded precursor populations have been identified in neuronal, myeloid, and adipocyte lineages (LeCouter et al., 1998; Vanderluit et al., 2004; Scime et al., 2005),

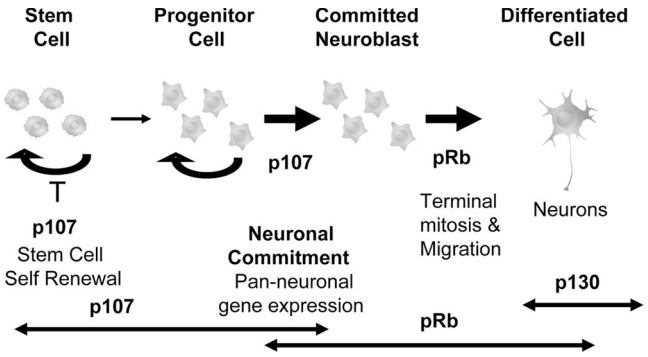

Figure 10. **Rb family members have distinct roles in neurogenesis.** In the progression from stem cell to differentiated neuron, Rb family members function sequentially to regulate each stage. In the neural precursor compartment, p107 performs two distinct functions. Within the neural stem cell population, p107 negatively regulates self-renewal, which ultimately affects the overall size of the neural precursor population. In the mature neural progenitor, p107 functions to promote commitment to a differentiated state. After neuronal commitment, Rb takes over to regulate terminal mitosis and migration of newly differentiated neurons. As cells become postmitotic, p130 functions to regulate cell survival (Liu and Greene, 2001; Liu et al., 2005).

our studies reveal a striking defect in the ability of progenitor cells to commit to a neuronal fate and undergo differentiation. Furthermore, the mechanism underlying this defect is through the deregulation of *Hes1*, an inhibitor of differentiation that functions by repressing the proneurogenic genes *Ngn1*, *Mash1*, and *NeuroD* (Sasai et al., 1992; Ishibashi et al., 1995). Collectively, these results reveal a novel function for p107 in promoting neural precursor cell commitment to a neuronal fate.

Rb family members perform distinct roles in neurogenesis

Collectively with our previous findings (Ferguson et al., 2002; Vanderluit et al., 2004), the results of this study reveal temporally sequential functions for Rb family proteins during the course of neural development (Fig. 10). First, p107 is expressed in proliferating neural precursor cells and controls the size of the neural precursor population. It does so by regulating neural precursor self-renewal and commitment to a neuronal fate. In the absence of p107, the progenitor pool is expanded by increased self-renewal and impairment in neuronal commitment. This function is unique for p107 because pRb-null mice do not exhibit an expanded population of neural precursor cells, nor do they show a decrease in neurogenesis (Ferguson et al., 2002). The temporal requirement for pRb occurs at the time of neuronal differentiation. Unlike p107-deficient animals, pRb-null progenitors successfully commit to a neuronal fate but exhibit impairment in migration and differentiation. This is evident by the widespread ectopic mitoses of committed progenitors throughout the developing cortex. Furthermore, committed neuroblasts derived from the ventral populations fail to migrate through their tangential trajectories to reach their final destinations in the dorsal telencephalon (Ferguson et al., 2002, 2005). Thus, as p107 becomes down-regulated, pRb plays an essential role to regulate differentiation and neuronal migration. Once neurons complete terminal differentiation, pRb becomes down-regulated, and p130 becomes the predominant Rb family member (Jiang et al., 1997;

Gill et al., 1998; Callaghan et al., 1999; Ferguson et al., 2000; Yoshikawa, 2000). Recent studies reveal that p130 is highly expressed in postmitotic cells and plays an important role in the regulation of neuronal survival (Liu and Greene, 2001; Liu et al., 2005). Thus, each Rb family protein plays a temporally distinct role that is crucial for normal neural development.

In conclusion, the key finding of this study is that p107, a cell cycle regulatory protein known for its role in controlling the cell cycle machinery, has a novel function in regulating the onset of differentiation. This new role provides insight as to how cell cycle proteins may participate in shaping the developing brain. We also show that deregulation of the Notch1 pathway is mechanistically important because deletion of a single allele of *Hes1* rescues the defects found in p107-deficient mice but has no effect on wild-type animals. In summary, we have identified a novel function for the cell cycle regulator p107 in promoting progenitor cell differentiation through regulation of the Notch–Hes1 signaling pathway.

Materials and methods

Mice

Germline p107-null mice were generated previously by LeCouter et al. (1998) and maintained on a mixed SV-129 and C57BL/6 background. Germline Hes1-null mice on an ICR background were originally generated by R. Kageyama (Ishibashi et al., 1995). Hes1/p107-deficient embryos were generated by interbreeding heterozygous ($Hes1^{+/-}$) mice with $p107^{+/-}$ mice. Animals were genotyped according to standard protocols with previously published primers for *p107* (LeCouter et al., 1998) and *Hes1* (Ishibashi et al., 1995). For embryonic time points, the time of plug identification was counted as E0.5. All experiments were approved by the University of Ottawa's Animal Care Ethics Committee, adhering to the guidelines of the Canadian Council on Animal Care.

Tissue fixation and cryoprotection

Pregnant dams and adult mice were killed with a lethal injection of sodium pentobarbitol. Embryos were dissected and submersion fixed overnight in 4% PFA in 1× PBS, pH 7.4. Adult mice were perfused with 1× PBS followed by cold 4% PFA, and brains were removed. Brains were postfixed overnight in 4% PFA, cryoprotected in 22% sucrose in 1× PBS, and frozen, and 14-μm coronal sections through the forebrain were collected on Superfrost Plus slides (Fisher Scientific).

In situ hybridization and quantitative real-time RT-PCR

Nonradioactive in situ hybridization and digoxigenin probe labeling was performed according to previously described protocols (Wallace and Raff, 1999). Antisense riboprobes for *Hes1* and *Hes5* were generated according to previously published sequences (Tomita et al., 1996). Total RNA was isolated from cortices from wild-type and p107-deficient embryos using TRIzol reagent according to the manufacturer's instructions (Invitrogen). RNA was reverse transcribed using the GeneAmp RNA PCR Core kit (Applied Biosystems). Real-time PCR was performed on cDNA using the TaqMan Universal PCR Master Mix (Applied Biosystems) with commercially provided PCR primers for *Hes1*, *Hes5*, and *glyceraldehyde-3-phoshpate dehydrogenase* from TaqMan Gene Expression Assays (Applied Biosystems).

Immunohistochemistry and Western blotting

Immunohistochemistry was performed on coronal cryostat sections from embryonic and adult brains with primary antibodies to mouse anti-NeuN (1:100; Chemicon), rabbit antiactive caspase-3 (1:500; BD Biosciences), rabbit anti-PH3 (1:400; Upstate Biotechnology), rat anti-BrdU (1:100; Accurate Chemicals), mouse anti-BrdU (1:100; Becton Dickinson), mouse anti-PCNA (1:300; Vector Laboratories), goat antidoublecortin (1:100; Santa Cruz Biotechnology, Inc.), mouse anti–βIII-tubulin (mouse monoclonal hybridoma supernatant; 1:100; Caccamo et al., 1989), and mouse anti-Nestin (1:400; Research Diagnostics). For BrdU birthdating experiments (E13.5–18.5), pregnant dams received a single injection of BrdU at 20 μg/g of body weight; for short-term BrdU incorporation experiments, pregnant dams and adult mice received intraperitoneal injections of BrdU at 100 μg/g of body weight. For BrdU detection, sections were denatured in 2 N HCl at 37°C for 15 min followed by neutralization in 0.1 M Na borate, pH 8.5, for 10 min at room temperature before incubation with the primary antibody. For PCNA detection, sodium citrate antigen retrieval, pH 6.0, was performed on sections before incubation with PCNA antibodies. In all double labeling with BrdU antibodies, denaturation and BrdU immunohistochemistry were performed after the first primary and secondary antibody incubation.

Protein was isolated from cultured neurospheres in lysis buffer, run on a 15% SDS-polyacrylamide gel, and transferred to a nitrocellulose membrane as described previously (Ferguson et al., 2000). Immunoblotting was performed with antibodies directed against Hes1 (provided by H. Kitamura, Yokohama City University School of Medicine, Yokohama, Japan; Ito et al., 2000), Hes5 (Chemicon), and actin (Santa Cruz Biotechnology, Inc.). Blots were developed by chemiluminescence according to the manufacturer's instructions (NEL100; PerkinElmer).

Cell counts and measurements

In the adult brain, $BrdU^+$ cells were counted along the entire length of the ventricular surface (dorsal and ventral) in every 10th section from the rostral crossing of the corpus callosum to the start of the third ventricle and crossing of the anterior commissure with an equal number of sections counted per brain as previously described (Morshead et al., 1998; Vanderluit et al., 2004). $PH3^+$ cells were counted along a 1,000-μm length of the ventricle in three representative sections through the forebrains of E10.5 embryos. In E13.5, 14.5, and 18.5 embryos, $BrdU^+$ cells and/or $NeuN^+$ cells were counted along a 750-μm length of the ventricle up through to the pial surface in four representative regions through the forebrain (Koutmani et al., 2004). Cortical plate, VZ, and cortical mantle measurements were performed on cresyl violet sections of E18 brains from wild type. Triplicate measurements were performed on three representative sections through the forebrain.

Promotor analysis

The *Hes1* promotor (1,270 bp) sequence, including a 224-bp 3′ sequence of the transcription start site, was amplified from mouse genomic DNA by PCR and inserted into a pGL3-Basic luciferase reporter construct (forward primer 5′-CGCGGCGGCAATAAAACATC-3′; reverse primer 5′-GATGAGTGCACAGGGGGAGAAAAGAGGTC-3′; Promega; Sasai et al., 1992; Takebayashi et al., 1994). To assess whether promotor activity was affected by p107, the pGL3B-Hes1 construct or the E2F-BS mutant (Hes1-3xBS) was cotransfected with expression vectors for either *p107* (pCMV-p107) or *Rb* (pGK-RB) into HEK 293A cells by standard calcium phosphate precipitation (Storring et al., 1999). 2 μg pMLV-LacZ was cotransfected with each sample to control for transfection efficiency. 4-methylumbelliferyl-D-galactoside assay was performed to standardize the transfection reaction, and luciferase activity was assessed according to standard procedures (Fortin et al., 2004). Statistical analysis was performed on the means of three different experiments.

Table I. **Primers for E2F-mutated Hes1 promotor construct**

	Forward	Reverse
Fragment 1	5′-ATCGGGTACCCGCGGGGCAATAAAACATC-3′	5′-TAGCAGATCTCCCTTACCGTCCC-3′
Fragment 2	5′-ATCGAGATCTGGGTTTAGTATCTCC-3′	5′-TAGCCTCGAGGCTTACGTCCTTTTACTTG-3′
Fragment 3	5′-ATCGCTCGAGGGATTCCAAAAATAAAATTC-3	5′-TAGCGCTAGCAAAGGAGTCCCGCTG-3′
Fragment 4	5′-ATCGGCTAGCACCTCGGGGTGAAATGG-3′	5′-TAGCAAGCTTCACGTACGGAATGCCAGC-3′

Primers were designed to exclude each of the three putative E2F-BSs, resulting in fragmentation of the Hes1 promotor into four pieces. Restriction sites were incorporated into primer ends to ease promotor reassembly.

Putative E2F consensus sites were identified by MatInspector software (Genomatix; Fig. 3 a). A mutant *Hes1* promotor minus all three E2F-binding sequences (Hes1-3xBS) was constructed by linking PCR fragments on each side of the E2F-BSs and inserting them into the pGL3B-luciferase construct (Table I).

Neurosphere assay

The neurosphere assay was performed on neuroepithelia from E10.5 embryos as previously described (Reynolds et al., 1992; Tropepe et al., 1999; Vanderluit et al., 2004). Statistical comparisons were performed on the mean number of neurospheres per embryo per genotype.

Microscopy

Sections treated for immunohistochemistry or in situ hybridization were examined by a microscope (Axioskop 2; Carl Zeiss MicroImaging, Inc.) with standard fluorescence and brightfield/darkfield settings at 5× NA 0.25 or 20× NA 0.50 objectives. Images were captured using a color video camera (Power HAD 3CCD; Sony) with Northern Eclipse software (Empix Imaging). For confocal microscopy, images were captured using a microscope (LSM 510 META; Carl Zeiss MicroImaging, Inc.) on an inverted microscope (Axiovert 200M; Carl Zeiss MicroImaging, Inc.) with the manufacturer's integrated digital imaging software. Figures were compiled using Photoshop 6.0 (Adobe). Manipulations of brightness and intensity were made equally to all treatment groups.

We thank W.C. McIntosh, Dominique Yelle, and Eric Ouellet for their invaluable technical assistance and expertise and Vladimir Ruzhynsky and Lisa Julian for critical review of this manuscript.

This work was supported by operating grants from the Canadian Institutes of Health Research to R.S. Slack. J.L. Vanderluit is a recipient of a fellowship from the Heart and Stroke Foundation of Canada. K.A. McClellan is supported by a Canada Graduate Doctoral Research Award from the Canadian Institutes of Health Research.

Submitted: 27 March 2007
Accepted: 31 May 2007

References

Caccamo, D., C.D. Katsetos, M.M. Herman, A. Frankfurter, V.P. Collins, and L.J. Rubinstein. 1989. Immunohistochemistry of a spontaneous murine ovarian teratoma with neuroepithelial differentiation. Neuron-associated beta-tubulin as a marker for primitive neuroepithelium. *Lab. Invest.* 60:390–398.

Callaghan, D.A., L. Dong, S.M. Callaghan, Y.X. Hou, L. Dagnino, and R.S. Slack. 1999. Neural precursor cells differentiating in the absence of Rb exhibit delayed terminal mitosis and deregulated E2F 1 and 3 activity. *Dev. Biol.* 207:257–270.

Caviness, V.S., Jr. 1982. Development of neocortical afferent systems: studies in the reeler mouse. *Neurosci. Res. Program Bull.* 20:560–569.

Caviness, V.S., Jr., T. Takahashi, and R.S. Nowakowski. 1995. Numbers, time and neocortical neuronogenesis: a general developmental and evolutionary model. *Trends Neurosci.* 18:379–383.

Cayre, M., J. Malaterre, S. Scotto-Lomassese, A. Aouane, C. Strambi, and A. Strambi. 2005. Hormonal and sensory inputs regulate distinct neuroblast cell cycle properties in adult cricket brain. *J. Neurosci. Res.* 82:659–664.

Cheng, T., N. Rodrigues, H. Shen, Y. Yang, D. Dombkowski, M. Sykes, and D.T. Scadden. 2000. Hematopoietic stem cell quiescence maintained by p21cip1/waf1. *Science*. 287:1804–1808.

Doetsch, F., J.M. Verdugo, I. Caille, A. Alvarez-Buylla, M.V. Chao, and P. Casaccia-Bonnefil. 2002. Lack of the cell-cycle inhibitor p27Kip1 results in selective increase of transit-amplifying cells for adult neurogenesis. *J. Neurosci.* 22:2255–2264.

Ferguson, K.L., S.M. Callaghan, M.J. O'Hare, D.S. Park, and R.S. Slack. 2000. The Rb-CDK4/6 signaling pathway is critical in neural precursor cell cycle regulation. *J. Biol. Chem.* 275:33593–33600.

Ferguson, K.L., J.L. Vanderluit, J.M. Hebert, W.C. McIntosh, E. Tibbo, J.G. MacLaurin, D.S. Park, V.A. Wallace, M. Vooijs, S.K. McConnell, and R.S. Slack. 2002. Telencephalon-specific Rb knockouts reveal enhanced neurogenesis, survival and abnormal cortical development. *EMBO J.* 21:3337–3346.

Ferguson, K.L., K.A. McClellan, J.L. Vanderluit, W.C. McIntosh, C. Schuurmans, F. Polleux, and R.S. Slack. 2005. A cell-autonomous requirement for the cell cycle regulatory protein, Rb, in neuronal migration. *EMBO J.* 24:4381–4391.

Fortin, A., J.G. MacLaurin, N. Arbour, S.P. Cregan, N. Kushwaha, S.M. Callaghan, D.S. Park, P.R. Albert, and R.S. Slack. 2004. The proapoptotic gene SIVA is a direct transcriptional target for the tumor suppressors p53 and E2F1. *J. Biol. Chem.* 279:28706–28714.

Gill, R.M., R. Slack, M. Kiess, and P.A. Hamel. 1998. Regulation of expression and activity of distinct pRB, E2F, D-type cyclin, and CKI family members during terminal differentiation of P19 cells. *Exp. Cell Res.* 244:157–170.

Hatakeyama, J., Y. Bessho, K. Katoh, S. Ookawara, M. Fujioka, F. Guillemot, and R. Kageyama. 2004. Hes genes regulate size, shape and histogenesis of the nervous system by control of the timing of neural stem cell differentiation. *Development*. 131:5539–5550.

Hitoshi, S., T. Alexson, V. Tropepe, D. Donoviel, A.J. Elia, J.S. Nye, R.A. Conlon, T.W. Mak, A. Bernstein, and D. van der Kooy. 2002. Notch pathway molecules are essential for the maintenance, but not the generation, of mammalian neural stem cells. *Genes Dev.* 16:846–858.

Ishibashi, M., K. Moriyoshi, Y. Sasai, K. Shiota, S. Nakanishi, and R. Kageyama. 1994. Persistent expression of helix-loop-helix factor HES-1 prevents mammalian neural differentiation in the central nervous system. *EMBO J.* 13:1799–1805.

Ishibashi, M., S.L. Ang, K. Shiota, S. Nakanishi, R. Kageyama, and F. Guillemot. 1995. Targeted disruption of mammalian hairy and Enhancer of split homolog-1 (HES-1) leads to up-regulation of neural helix-loop-helix factors, premature neurogenesis, and severe neural tube defects. *Genes Dev.* 9:3136–3148.

Ito, T., N. Udaka, T. Yazawa, K. Okudela, H. Hayashi, T. Sudo, F. Guillemot, R. Kageyama, and H. Kitamura. 2000. Basic helix-loop-helix transcription factors regulate the neuroendocrine differentiation of fetal mouse pulmonary epithelium. *Development*. 127:3913–3921.

Jiang, Z., E. Zacksenhaus, B.L. Gallie, and R.A. Phillips. 1997. The retinoblastoma gene family is differentially expressed during embryogenesis. *Oncogene*. 14:1789–1797.

Kageyama, R., T. Ohtsuka, J. Hatakeyama, and R. Ohsawa. 2005. Roles of bHLH genes in neural stem cell differentiation. *Exp. Cell Res.* 306:343–348.

Kippin, T.E., D.J. Martens, and D. van der Kooy. 2005. p21 loss compromises the relative quiescence of forebrain stem cell proliferation leading to exhaustion of their proliferation capacity. *Genes Dev.* 19:756–767.

Koutmani, Y., C. Hurel, E. Patsavoudi, M. Hack, M. Gotz, D. Thomaidou, and R. Matsas. 2004. BM88 is an early marker of proliferating precursor cells that will differentiate into the neuronal lineage. *Eur. J. Neurosci.* 20:2509–2523.

LeCouter, J.E., B. Kablar, W.R. Hardy, C. Ying, L.A. Megeney, L.L. May, and M.A. Rudnicki. 1998. Strain-dependent myeloid hyperplasia, growth deficiency, and accelerated cell cycle in mice lacking the Rb-related p107 gene. *Mol. Cell. Biol.* 18:7455–7465.

Liu, D.X., and L.A. Greene. 2001. Neuronal apoptosis at the G1/S cell cycle checkpoint. *Cell Tissue Res.* 305:217–228.

Liu, D.X., N. Nath, S.P. Chellappan, and L.A. Greene. 2005. Regulation of neuron survival and death by p130 and associated chromatin modifiers. *Genes Dev.* 19:719–732.

McClellan, K.A., and R.S. Slack. 2006. Novel functions for cell cycle genes in nervous system development. *Cell Cycle*. 5:1506–1513.

Molofsky, A.V., R. Pardal, T. Iwashita, I.K. Park, M.F. Clarke, and S.J. Morrison. 2003. Bmi-1 dependence distinguishes neural stem cell self-renewal from progenitor proliferation. *Nature*. 425:962–967.

Molofsky, A.V., S. He, M. Bydon, S.J. Morrison, and R. Pardal. 2005. Bmi-1 promotes neural stem cell self-renewal and neural development but not mouse growth and survival by repressing the p16Ink4a and p19Arf senescence pathways. *Genes Dev.* 19:1432–1437.

Morshead, C.M., and D. van der Kooy. 1992. Postmitotic death is the fate of constitutively proliferating cells in the subependymal layer of the adult mouse brain. *J. Neurosci.* 12:249–256.

Morshead, C.M., C.G. Craig, and D. van der Kooy. 1998. In vivo clonal analyses reveal the properties of endogenous neural stem cell proliferation in the adult mammalian forebrain. *Development*. 125:2251–2261.

Ohtsuka, T., M. Sakamoto, F. Guillemot, and R. Kageyama. 2001. Roles of the basic helix-loop-helix genes Hes1 and Hes5 in expansion of neural stem cells of the developing brain. *J. Biol. Chem.* 276:30467–30474.

Reynolds, B.A., W. Tetzlaff, and S. Weiss. 1992. A multipotent EGF-responsive striatal embryonic progenitor cell produces neurons and astrocytes. *J. Neurosci.* 12:4565–4574.

Sasai, Y., R. Kageyama, Y. Tagawa, R. Shigemoto, and S. Nakanishi. 1992. Two mammalian helix-loop-helix factors structurally related to *Drosophila* hairy and Enhancer of split. *Genes Dev.* 6:2620–2634.

Scime, A., G. Grenier, M.S. Huh, M.A. Gillespie, L. Bevilacqua, M.E. Harper, and M.A. Rudnicki. 2005. Rb and p107 regulate preadipocyte differentiation into white versus brown fat through repression of PGC-1alpha. *Cell Metab.* 2:283–295.

Stevaux, O., and N.J. Dyson. 2002. A revised picture of the E2F transcriptional network and RB function. *Curr. Opin. Cell Biol.* 14:684–691.

Storring, J.M., A. Charest, P. Cheng, and P.R. Albert. 1999. TATA-driven transcriptional initiation and regulation of the rat serotonin 5-HT1A receptor gene. *J. Neurochem.* 72:2238–2247.

Takahashi, T., T. Goto, S. Miyama, R.S. Nowakowski, and V.S. Caviness Jr. 1999. Sequence of neuron origin and neocortical laminar fate: relation to cell cycle of origin in the developing murine cerebral wall. *J. Neurosci.* 19:10357–10371.

Takebayashi, K., Y. Sasai, Y. Sakai, T. Watanabe, S. Nakanishi, and R. Kageyama. 1994. Structure, chromosomal locus, and promoter analysis of the gene encoding the mouse helix-loop-helix factor HES-1. Negative autoregulation through the multiple N box elements. *J. Biol. Chem.* 269:5150–5156.

Tomita, K., M. Ishibashi, K. Nakahara, S.L. Ang, S. Nakanishi, F. Guillemot, and R. Kageyama. 1996. Mammalian hairy and Enhancer of split homolog 1 regulates differentiation of retinal neurons and is essential for eye morphogenesis. *Neuron*. 16:723–734.

Tropepe, V., M. Sibilia, B.G. Ciruna, J. Rossant, E.F. Wagner, and D. van der Kooy. 1999. Distinct neural stem cells proliferate in response to EGF and FGF in the developing mouse telencephalon. *Dev. Biol.* 208:166–188.

Vanderluit, J.L., K.L. Ferguson, V. Nikoletopoulou, M. Parker, V. Ruzhynsky, T. Alexson, S.M. McNamara, D.S. Park, M. Rudnicki, and R.S. Slack. 2004. p107 regulates neural precursor cells in the mammalian brain. *J. Cell Biol.* 166:853–863.

Wallace, V.A., and M.C. Raff. 1999. A role for Sonic hedgehog in axon-to-astrocyte signalling in the rodent optic nerve. *Development*. 126:2901–2909.

Yoshikawa, K. 2000. Cell cycle regulators in neural stem cells and postmitotic neurons. *Neurosci. Res.* 37:1–14.

Yuan, Y., H. Shen, D.S. Franklin, D.T. Scadden, and T. Cheng. 2004. In vivo self-renewing divisions of haematopoietic stem cells are increased in the absence of the early G1-phase inhibitor, p18INK4C. *Nat. Cell Biol.* 6:436–442.